Crystal Structure and Composition of Poly(ethylene terephthalate-*co*-4,4′-bibenzoate)

Hongming Ma,[†] Tetsuya Uchida,[‡,⊥] David M. Collard,[†] David A. Schiraldi,[§] and Satish Kumar*[,‡]

School of Chemistry and Biochemistry, Georgia Institute of Technology, Atlanta, Georgia 30332-0400; School of Polymer, Textile and Fiber Engineering, Georgia Institute of Technology, Atlanta, Georgia 30332-0295; and Department of Macromolecular Science and Engineering, Case Western Reserve University, Cleveland, Ohio 44106

Received June 29, 2004; Revised Manuscript Received August 8, 2004

ABSTRACT: The crystal structure in random copolymers poly(ethylene terephthalate-*co*-4,4′-bibenzoate) (PET/BB) was studied using wide-angle X-ray diffraction (WAXD). The composition of crystalline and amorphous regions has been studied by FTIR spectroscopy using the amorphous peaks at 1580 and 1560 cm^{-1} for terephthalate (T) and bibenzoate (B) units, respectively. Further, PET/BB55 was hydrolyzed to selectively etch the amorphous regions. The hydrolyzed products were further studied by FTIR and ^1H NMR spectroscopy, wide-angle X-ray diffraction, and transmission electron microscopy. Results show that crystal structures are very close to that of the respective homopolymer, PET and poly(ethylene bibenzoate) (PEBB) for the low and high BB content samples, respectively. The crystalline region of high BB content fibers is composed of mainly PEBB units. In PET/BB55 fiber, among the 30 wt % of the copolymer which was not etched, there is only one terephthalate unit for every five repeat units of bibenzoate. The crystal size of B type crystals along the *c* axis was found to be around five repeat units long. Short chain segments rich in BB are sufficient to induce crystallization, to form PEBB-like crystals.

Introduction

Poly(ethylene terephthalate-*co*-4,4′-bibenzoate) (PET/BB) copolymers crystallize across the entire composition range, especially upon orientation and annealing.[1] PET/BB copolymers with 45, 55, and 65 mol % of bibenzoate comonomer (PET/BB45, -55, and -65, respectively) exhibit liquid crystalline polymer-like behaviors during melt spinning.[2] The fibers obtained from these polymers at low take-up speeds (i.e., a few hundred m/min) exhibit maximum achievable orientation and have modulus values in the range 35−45 GPa, approaching the value for thermotropic liquid crystalline copolyester Vectra (a copolyester of 1-hydroxy-4-benzoic acid and 2-hydroxy-6-naphthoic acid, HNA/HBA 75/25).[3] On the other hand, fibers of PET and PET/BB5, -15, and -35 obtained under the same conditions are amorphous and unoriented, and drawing at 110−125 °C must be applied to achieve high levels of orientation. Even then, the moduli of the second group of fibers are around 10 GPa. Fibers of PET/BB45, -55, and -65 also have much better retention of modulus at elevated temperatures than fibers of PET and copolyesters with low BB content.[1] Given the strong influence of BB units on the PET/BB fiber properties, we set out to examine the structure and morphology of PET/BB fibers. The crystal structure and composition of these copolymers are the subjects of the current study.

Cocrystallization of aromatic and semiaromatic copolyesters has been a subject of intensive research.[4−9] Differences in the length of the comonomer unit and the conformational flexibility were found to be critical for cocrystallization.[10] Windle and co-workers proposed a nonperiodic layer (NPL) model for the HNA/HBA system.[7−9] This model extended more generally to semiaromatic copolyester poly(ethylene 4,4′-bibenzoate-*co*-2,6-naphthalate) (PEN/BB)[4] and poly(ethylene terephthalate-*co*-2,6-naphthalate) (PET/N).[11,12] The model suggests that these random copolymers crystallize by segregation and lateral matching of identical sequences. The crystals therefore contain both comonomers to form a layered structure without periodicity along the chain direction. By implication, the NPL model suggests that the composition of the crystalline region would be comparable to that of the copolymer.

In this paper we have studied the variation of crystallinity, crystal structure, and monomer distribution among the two phases as a function of PET/BB copolymer composition. PET has been selectively hydrolyzed to remove amorphous regions and to preserve the crystals.[13,14] A similar procedure has been used in the present work to selectively remove the amorphous regions of PET/BB55, thus allowing the composition of the crystalline and amorphous regions to be elucidated and crystal structure to be identified.

Experimental Section

Poly(ethylene terephthalate-*co*-4,4′-bibenzoate) copolymers were made by 285−310 °C melt polymerization of dimethyl terephthalate, dimethyl 4,4′-bibenzoate, and ethylene glycol in the presence of antimony oxide catalyst, as was previously described.[15] The degree of copolymer randomness and fiber spinning conditions for PET/BB were reported in a previous study.[1] Wide-angle X-ray diffraction (WAXD) was carried out on a Rigaku MicroMax 002 (XBG) system operating at 45 kV and 0.66 mA using Cu Kα irradiation. Air scattering was subtracted after making a correction for absorption by the sample. Data processing were carried out using MDI Jade 6.1. A linear background was fitted for all the curves. Profile fittings were repeated until the residual error of fit was less

[†] School of Chemistry and Biochemistry, Georgia Institute of Technology.
[‡] School of Polymer, Textile and Fiber Engineering, Georgia Institute of Technology.
[§] Case Western Reserve University.
[⊥] Current address: Faculty of Engineering, Okayama University, Okayama 700-8530, Japan.
* Corresponding author: e-mail satish.kumar@ptfe.gatech.edu.

10.1021/ma0486905 CCC: $27.50
Published on Web 09/10/2004

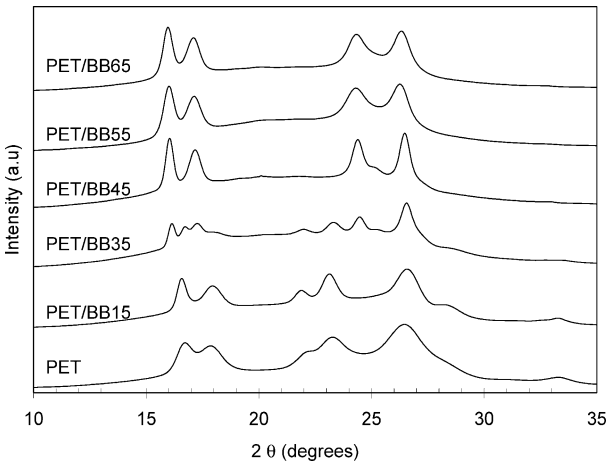

Figure 1. WAXD of PET and PET/BB bulk copolymers.

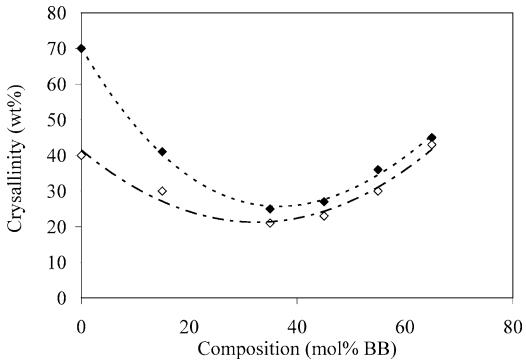

Figure 2. Crystallinity in PET/BB copolymers as measured by the X-ray method: solid symbol, annealed bulk polymer; open symbol, heat-treated fibers.

than 2%. Crystal size was calculated by using the Scherrer equation,[16] with a *K* value of 0.9 rad. Crystallinity was determined from the ratio of the peak area for crystalline peaks and the total area under the radial scan curves.[17]

Hydrolytic etching was carried out on PET/BB55 fibers. A mixture of water (50 mL) and fiber (0.86 g) was heated to 160 °C for 60 h in an autoclave with a poly(tetrafluoroethylene) liner. The solid product was removed by filtration and washed with dimethyl sulfoxide (DMSO). IR spectra of the pristine fiber and hydrolyzed materials were obtained on a Perkin-Elmer Spectrum One FTIR spectrometer. ^{1}H NMR spectra were obtained using a Varian Mercury Vx 300 spectrometer. The fiber and the DMSO-insoluble part were dissolved in trifluoroacetic acid-d_1, while the DMSO-soluble fraction was recorded in dimethyl sulfoxide-d_6. Samples for transmission electron microscopy were prepared by depositing the aqueous suspension of the DMSO-insoluble part onto carbon grids. Bright field images and selected area electron diffraction (SAED) patterns were collected on a JEM 4000 EX operated at 400 kV. The TEM camera length was calibrated by using gold electron diffraction.

Results and Discussion

X-ray Diffraction on Unorientated Samples. Wide-angle X-ray diffraction of annealed bulk PET and PET/BB copolymers are shown in Figure 1. The scans clearly indicate the crystalline nature of the copolymers across the whole composition range. Crystallinity values determined from X-ray diffraction are plotted in Figure 2. The diffraction scan of PET/BB15 is similar to that of the PET. On the other hand, the scans of PET/BB45, -55, and -65 are comparable to each other and match the diffraction patterns of poly(ethylene bibenzoate) (PEBB).[18] For PET/BB35, diffraction peaks corresponding to the crystal structures of both PET and PEBB can be seen. These observations suggest that the crystal packing changes from that of PET to PEBB with increasing bibenzoate content, and in PET/BB35 both PET and PEBB crystals coexist. Hereafter, we refer the PET-like crystals as "T" type crystal and PEBB-like crystal structure as "B" type crystal. The indexing for PET and PEBB homopolymer was used for T type unit cells and B type unit cells, respectively. The *d* spacings observed for PET/BB copolymers are listed in Table 1 for T type crystal structure and Table 2 for B type crystal structure. The presence of (101) and (110) diffraction peaks indicates that the crystal has a 3-D structure. For both crystal structures, the *d* spacings change gradually with increasing bibenzoate content, which may be due to the incorporation of BB unit into T crystals or T unit incorporation into B crystals. Using the unit cell parameters of PET[19] ($a = 4.508$, $b = 5.882$, $c = 10.787$, $\alpha = 100.01$, $\beta = 118.36$, $\gamma = 110.56$) and PEBB[18] ($a = 5.75$, $b = 3.82$, $c = 14.62$, $\alpha = 90.1$, $\beta = 90.3$, $\gamma = 78.1$) as well as various *d* spacings in Tables 1 and 2, the unit cell parameters for PET/BB copolymer for both T and B type crystals were calculated and are given in Figure 3. The lengths of *a* and *b* axes in both T and B type crystals vary as the composition changes, but there is a clear difference in lattice parameters between the two types of crystals. It is understandable that different comonomers may be able to enter the crystal of different type. Along the chain direction, the length of the *c*-axis would change continuously if the copolymer were to crystallize by sequence matching model (NPL), as is the case for PET/N.[11] However, in PET/BB copolymers (Figure 3c), there is a transition from T to B type crystals at 35 mol % of BB. For PET/BB35 two crystal forms coexist. The length of the *c* axis in T type crystal increases by the addition of the B comonomer. However, the *c*-axis length of B crystals does not change significantly with the addition of T. These results suggest that in PET/BB copolymers the T and B units do not cocrystallize in the same ratio as the copolymer composition.

Table 1. *d* Spacings (in Å) for T Type Crystals in PET/BB Unoriented Samples

polymer	$(0\bar{1}1)$	(010)	$(\bar{1}10)$	(100)
PET	5.447(3)	5.028(6)	3.898(5)	3.392(8)
PET/BB15	5.454(1)	5.013(7)	3.898(6)	3.471(3)
PET/BB35	5.432(4)	4.983(4)	3.886(4)	3.473(2)

Table 2. *d* Spacings (in Å) for B Type Crystals in PET/BB Unoriented Samples; for Comparison PEBB *d* Spacings from the Literatures Are Also Given

polymer	(100)	(101)	(010)	(110)
PET/BB35	5.490(2)	5.149(1)	3.634(1)	3.356(1)
PET/BB45	5.523(1)	5.159(1)	3.648(1)	3.365(1)
PET/BB55	5.563(1)	5.193(2)	3.665(1)	3.378(2)
PET/BB65	5.549(1)	5.208(2)	3.667(1)	3.386(1)
PEBB[18]	5.628	5.252	3.699	3.404
PEBB[4]	5.545	5.206	3.651	3.377

X-ray Diffraction of Fibers Wide-angle X-ray diffraction scans of PET/BB fibers are shown in Figure 4. The fiber crystal structure can also be divided into two groups: PET/BB15 and -35 have T type crystals, and PET/BB45, -55, and -65 fibers have B type crystals. However, the $(0\bar{1}1)$, (010) in PET and low BB content fibers and (010), (110) peaks in high BB content fibers merged due to limited crystal size.

Meridian scans of PET/BB45, -55, and -65 fibers are plotted in Figure 5. Diffraction peaks at 14.71, 7.34, and

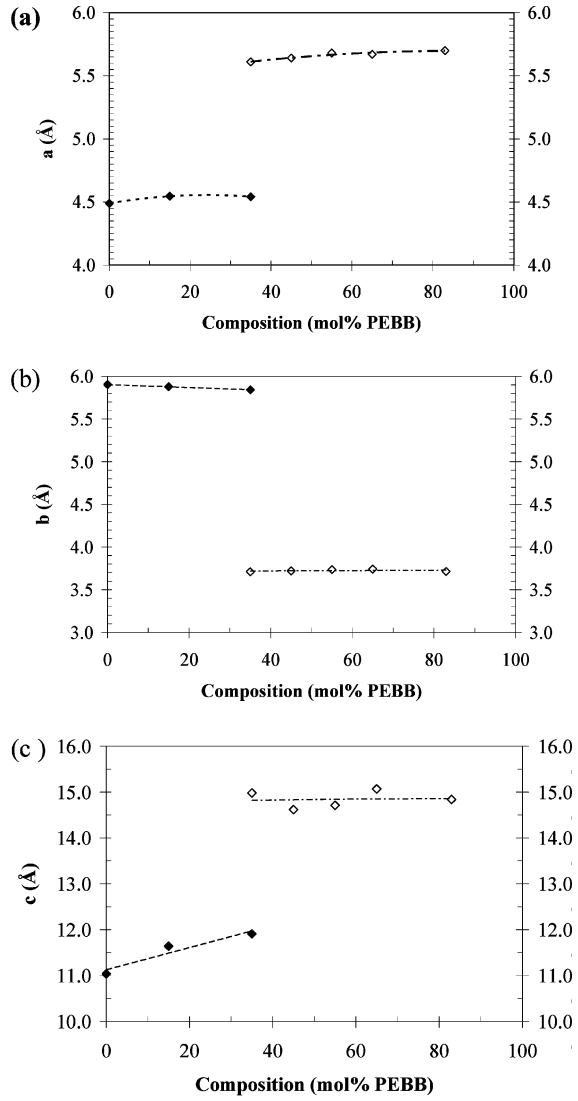

Figure 3. PET/BB unit cell parameters as a function of copolymer composition.

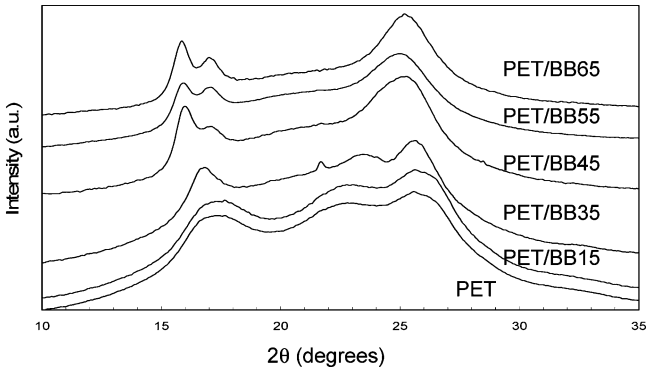

Figure 4. WAXD of PET and PET/BB fibers.

2.95 Å corresponding to the (001), (002), and (005) diffractions of PEBB can be seen. The crystal thickness of B type crystal structure along the chain direction determined from the (001) peak using the Scherrer equation is 75 Å, which corresponds to the length of about five PEBB repeat units. In addition, aperiodic streaks are seen in the meridian. These narrow and high-intensity streaks (at 2θ of 26.3° and 46.6°) are a prominent feature in the meridional direction of the high BB content fibers. The 3.5 Å spacing of the

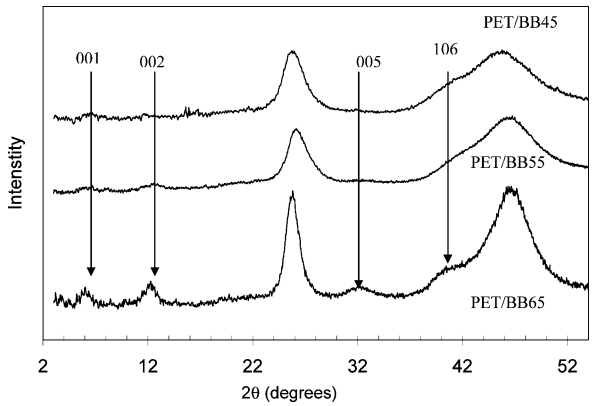

Figure 5. WAXD meridional scans of PET/BB fiber.

horizontal streak in PET/BB55 fiber is less than the expected spacing of the (004) plane for PEBB (3.65 Å). Similar horizontal streaks were observed in many rigid rode polymers as well as in semiaromatic polyester fibers.[11] The origin of streaks has been ascribed to diffraction from a single chain.

To further examine the origin of the streaks, a noncrystalline but oriented PET/BB55 fiber was processed by stretching amorphous PET/BB55 fiber at room temperature (T_g = 105 °C). The WAXD of this fiber shows no diffraction in the equatorial but horizontal streaks in the meridional direction. Upon annealing, a strong equatorial peak emerged and the meridional streaks were preserved. The streaks disappeared when the fiber was heated to ∼200 °C, while the diffraction pattern of the crystal survived. These observations suggest that the streaks in PET/BB45, -55, and -65 fibers originate from the oriented chains in the amorphous regions rather than from the crystals. The crystalline regions in high BB content fibers give sharp periodic diffractions spots, while the amorphous region gives aperiodic diffraction streaks. The streaks are dominated in intensity due to large volume fraction of the amorphous regions. A similar situation was found in a wholly aromatic copolyester fiber composed of *p*-hydroxybenzoic acid, 4,4′-dihydroxybiphenyl, terephthalic acid, and isophthalic acid, where both diffraction spots and horizontal streaks in the meridional direction were observed.[20] The diffraction spots came from the PHB crystals, and the streaks originated from the disordered chains.

From X-ray analysis, we conclude that in high BB content fiber the crystals are formed by relatively pure PEBB units rather than by sequence matching and uniform incorporation of random sequence as in the case of PET/PEN copolymer.[11,12] The difference in the *c*-axis length between T (10.75 Å) and B (14.62 Å) crystals is significant, which may not be easily compensated by rotation of the ethylene glycol unit. To determine the composition of the crystallites in the copolymers, spectroscopy and hydrolytic etching studies were carried out.

Vibration Spectroscopy. FTIR can be applied to estimate the composition of the crystalline and amorphous regions of PET/BB fibers. The V_{8a} vibration of the phenyl ring is IR-inactive in the crystalline state since the conformation of the terephthalate unit is symmetric to the inversion center. However, in the amorphous regions the chains deviate from their symmetric position, and the V_{8a} motion becomes IR-active with absorption at 1580 cm^{-1}; thus, this peak is only characteristic of the terephthalate rings in the amor-

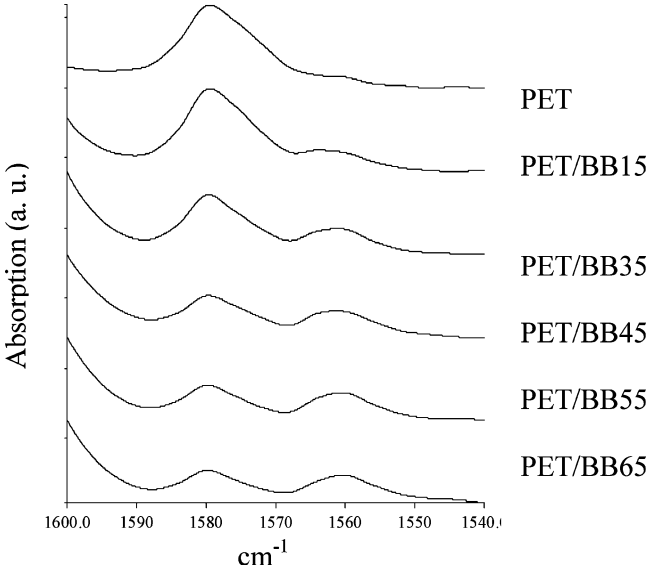

Figure 6. FTIR spectra of PET and PET/BB fibers in the vicinity of the V_{8a} absorption region.

phous regions.[21,22] Similarly, because of the centrosymmetric nature of the PEBB crystal structure,[18] the same situation occurs with respect to bibenzoate units. The peak at 1560 cm^{-1} indicates biphenyl rings in the amorphous regions. FTIR spectra of PET and PET/BB fibers are shown in Figure 6. In PET there is only one peak at 1580 cm^{-1}. With the incorporation of BB a new peak appears at 1560 cm^{-1}, and its intensity increases with increasing BB content. The ratio of these two peaks gives the relative concentration of the two monomers in the amorphous regions. Combined with the crystallinity data (Figure 2), the distribution of repeat units in the amorphous and crystalline regions was calculated (Table 3). These results show that in low BB content fibers the BB units are located mainly in the amorphous region. However, in high BB content fibers, the crystalline region is rich in BB units, and the amorphous region has both BB and T units.

Table 3. Monomer Distribution (mol %) in the Amorphous and Crystalline Regions

sample	crystallinity, wt %	$A^a_{1560}/A_{(1560+1579)}$	amorphous region		crystalline region	
			B	T	B	T
PET	40	0	0	60	0	40
PET/BB15	30	0.12	10	65	5	20
PET/BB35	21	0.30	30	60	5	15
PET/BB45	23	0.40	30	50	15	5
PET/BB55	30	0.43	30	40	25	5
PET/BB65	43	0.52	30	30	35	5

[a] Area under the peak.

Hydrolysis. To further study the composition in the crystalline region, PET/BB55 fiber was subjected to hydrolysis study. Hydrolysis conditions were chosen on the basis of previous reports of the hydrolytic etching of semicrystalline PET in which weight loss and lamella thickness level off after 50 h.[14] Under these conditions, it is expected that only the amorphous regions are hydrolyzed and that the crystalline regions remain intact. After hydrolysis, 32 wt % of DMSO-insoluble solid was obtained with a degree of crystallinity of 87 wt %.

The IR spectrum of the DMSO-insoluble part (Figure 7b) resembles that of the fiber (Figure 7a). The absorption at 1750−1720 cm^{-1} (carbonyl stretching), 1200−1150 cm^{-1} (CO−O stretching), and 1100−1050 cm^{-1} (O−CH_2 stretch) are characteristic of main chain polyesters. The absorptions at 1370 and 1340 cm^{-1} arise from the ethylene glycol wagging in gauche and trans conformations, respectively. However, the prominence of O−H stretching at 3600 cm^{-1}, broadening of the carbonyl stretching vibration to lower frequency, and the decreased absorbance at 1100 cm^{-1} with respect to the spectrum of the fiber indicates decrease in chain length. The trans/gauche ratio increased upon hydrolysis (indicated by the ratio of the absorbance at 1370 and 1340 cm^{-1}), consistent with selective etching of the amorphous regions as the gauche conformation only exists in the amorphous regions. The spectrum of the DMSO-soluble part (Figure 7c) shows the bands at 2850

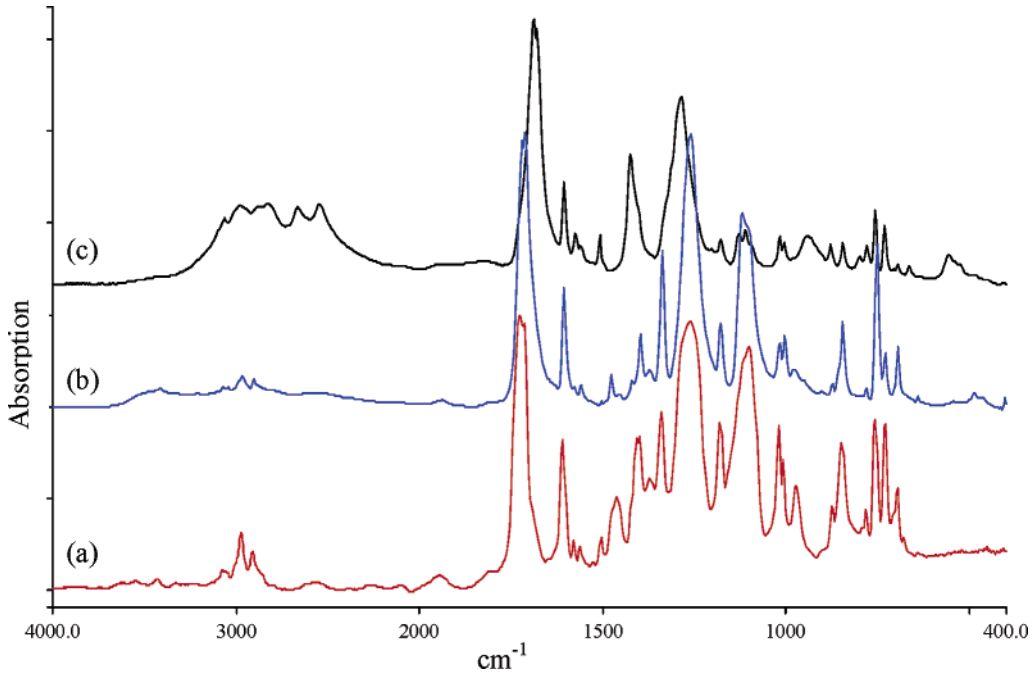

Figure 7. FTIR spectra of (a) PET/BB55 fiber, (b) DMSO-insoluble part, and (c) DMSO-soluble part.

Table 4. *d* Spacings (in Å) of DMSO-Insoluble Part Obtained from X-ray and Electron Diffraction; for Comparison Literature Values Are Also Given

hkl	$d_{obs,X-ray}$	$d_{obs,ED}$	Li, Brisse[18]	Lu, Windling[4]
100	5.58		5.62	5.54
010	3.65	3.7	3.69	3.65
110	3.37		3.44	3.37
101, $\bar{1}$01	5.21	5.2	5.26	5.2
11$\bar{1}$		3.3	3.32	
1$\bar{1}$1		2.7	2.80	
$\bar{1}$02	4.44		4.43	4.53
002	7.53		7.36	8.71
201	2.75		2.78	
202		2.6	0.263	
212	2.33		2.34	
007	2.06		2.06	
300	1.85			

Table 5. Comparison of Crystal Thickness (in Å) before and after Hydrolysis

hkl	100	101	001
PET/BB55 fiber	96	73	75
DMSO-insoluble part	150	78	71

and 1650 cm^{-1}, which are characteristic of aromatic carboxylic acid. The ethylene glycol CH_2 wagging mode at 1370 and 1340 cm^{-1} and the ester $O-CH_2$ stretch at 1018 cm^{-1} are all absent, suggesting that the hydrolysis byproducts are mainly low molecular weight acids. The ethylene glycol produced by hydrolysis was removed during evaporation of the DMSO.

^{1}H NMR was used to quantify the comonomer composition in different samples. PET/BB55 has a phenyl-to-biphenyl ratio of 45 to 55 and aromatic-to-aliphatic ratio of 1 to 1. The DMSO-soluble part has a phenyl/biphenyl ratio of 52 to 48 and lack of aliphatic units. For the DMSO-insoluble part the ratio between phenyl and biphenyl unit is 17:83, and the ratio between aromatic units to ethylene glycol units is close to 1:1. These results suggest that in the DMSO-insoluble part there is only one T unit per fiver repeat units of BB. A small amount of terephthalate units might be incorporated inside the crystals or lie between the lamella planes. In PET, it has been shown that hydrolytic etching is inefficient to remove the intralamellar segments.[13]

The *d* spacings of the DMSO-insoluble part (Table 4) match those of the PEBB crystal.[4,18] Thus, the DMSO-insoluble portion consists mainly of crystal lamellae of PEBB. The mass balance and crystallinity of the DMSO-insoluble fraction corresponds to a weight percent crystallinity in the pristine fiber of 29%. This is in good agreement with the X-ray crystallinity index of the pristine fiber prior to hydrolysis (30%). The PET/BB55 polymer annealed at 210 °C for 10 h shows crystallinity of 32%. Assuming that no significant increase in crystallinity took place during the hydrolysis, these results suggest that the hydrolysis is selective for ester linkages in the amorphous regions. The crystal thickness normal to (100), (101), and (001) diffraction planes for PET/BB55 fiber and that of the DMSO-insoluble part are compared in Table 5. The crystal thickness normal to the (100) plane increased significantly upon hydrolysis, which may be due to lateral aggregation of crystallites. However, crystal thickness in the (101) and (001) normal directions did not change. This is expected as chains are being cut, and the crystal size cannot increase along the chain direction.

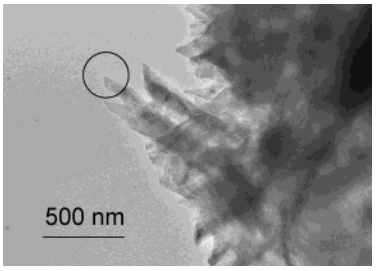

Figure 8. Transmission electron micrograph of the DMSO-insoluble part from hydrolyzed PET/BB55 fiber.

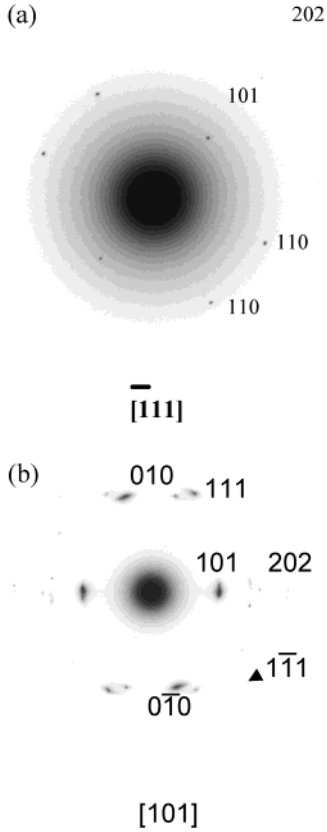

Figure 9. Selected area electron diffraction from isolated lamellar crystals obtained by hydrolytic etching of PET/BB55 fiber: (a) $\bar{1}$11 and (b) 101 diffractions.

A TEM image of lamellar aggregate is shown in Figure 8. Electron diffraction (Figure 9a) on an isolated lamella (as indicated by the circle in Figure 8) can be assigned by using the unit cell of the PEBB crystal (Table 4). The pattern suggests that the view direction is the $\bar{1}$11 direction and that the lamella is composed of (100) twinned crystallites. The diffraction pattern from the 101 direction (Figure 9b) can also be assigned to a PEBB unit cell. These results further confirm that the crystal structure of BB-rich PET/BB copolymers is dominated by PEBB units. The terephthalate units, observed by FTIR, most probably lie between the lamellar crystals.

Conclusions

From the above crystal structure and composition analyses we conclude that PET/BB random copolymers crystallize into either T or B type crystals depending on the copolymer composition. Comonomer composition of the crystalline region is substantially different than the overall copolymer composition. If the crystallization

were to occur by random sequence matching, then the composition of the crystals would be comparable to the overall copolymer composition. In high BB content copolymers, chain segments rich in BB yet random, e.g., "TBBTBBB", aggregate and crystallize to form B crystals with a small amount of T units being included. The probability of finding this type of chain segments in random PET/BB45 to 65 is significant. Crystals thus formed has short thickness along the chain, which indicates that lateral aggregation of BB segments of only 2−3 repeat units may have formed thermodynamically stable nuclei.

Homopolymers of 4,4′-bibenzoate and various diols have been shown to be liquid crystalline.[18,23−27] Mesophase and transient liquid crystallinity have been reported in PET[28−31] and PET/N copolymers.[32] We observed a transient, highly birefringent, and mobile phase for PET/BB45 at 210 °C, upon cooling from the isotropic melt.[1] Spinning behavior and mechanical properties of PET/BB45, -55, and -65 suggest the formation of a liquid crystalline phase. With the increased chain rigidity, as a result of addition of bibenzoate unit, it is possible that few homosequences of BB aggregate in the melt, which than crystallize into thin platelike crystals. Thus, a structured melt formed during melt spinning could provide for better fiber orientation. The resulting structure imparts superior physical properties to fibers. We will show in a following paper that the amorphous chains in high BB content PET/BB fiber indeed have much better orientation than that of PET and low BB content fibers.

Acknowledgment. The authors are grateful to Kosa (Spartanburg, SC) for the PET/BB copolymers and for financial support of this study. Special thanks are due to Dr. Tao Liu for many insightful discussions and help in calculating lattice parameters. NMR measurements by Drs. T. J. Zhao and L. Li are highly appreciated.

References and Notes

(1) Ma, H.; Hibbs, M.; Collard, D. M.; Kumar, S.; Schiraldi, D. A. *Macromolecules* **2002**, *35*, 5123.
(2) Beer, D.; Ramirez, E. *J. Text. Inst.* **1990**, *4*, 81.
(3) Beer, D.; Ramirez, E. *J. Text. Inst.* **1990**, *4*, 81.
(4) Wendling, J.; Gusev, A. A.; Suter, U. W.; Braam, A.; Leemans, L.; Meier, J. R.; Aerts, J.; Heuvel, J. v. d.; Hottenhuis, M. *Macromolecules* **1999**, *32*, 7866.
(5) Wendling, J.; Suter, U. W. *Macromolecules* **1998**, *31*, 2509.
(6) Wendling, J.; Suter, U. W. *Macromolecules* **1998**, *31*, 2516.
(7) Hanna, S.; Winle, A. H. *Polymer* **1988**, *29*, 207.
(8) Golombok, R.; Hanna, S.; Windle, A. H. *Mol. Cryst. Liq. Cryst.* **1988**, *155*, 281.
(9) Hanna, S.; Romo-Uribe, A.; Windle, A. H. *Nature (London)* **1993**, *366*, 546.
(10) Hachiboshi, M.; Fukuda, T.; Kobayashi, S. *J. Macromol. Sci., Phys.* **1969**, *B3*, 525.
(11) Lu, X.; Windle, A. H. *Polymer* **1995**, *36*, 451.
(12) Lu, X.; Windle, A. H. *Polymer* **1996**, *37*, 2027.
(13) Baltà Calleja, F. J.; Cagiao, M. E. *J. Mcromol. Sci., Phys.* **1994**, *B33*, 333.
(14) Miyagi, A.; Wunderlich, B. *J. Polym. Sci., Phys.* **1972**, *10*, 2073.
(15) Schiraldi, D. A.; Lee, J. J.; Gould, S. A. C.; Occelli, M. L. *J. Ind. Eng. Chem.* **2000**, *7*, 67.
(16) Klug, H. P.; Alexander, L. E. *X-Ray Diffraction Procedures*; Wiley: New York, 1954; Chapter 3.
(17) Alexander, L. E. *X-Ray Diffraction Methods in Polymer Science*; John Wiley & Sons: New York, 1969; Chapter 9.
(18) Li, X.; Brisse, F. *Macromolecules* **1994**, *27*, 2276.
(19) Fu, Y.; Busing, W. R.; Jin, Y.; Affholter, K. A.; Winderlich, B. *Macromolecules* **1993**, *26*, 2187.
(20) Uchida, T.; Shimamura, K. *Polym. Adv. Technol.* **2000**, *11*, 198.
(21) Liang, C. Y.; Krimm, S. *J. Mol. Spectrosc.* **1959**, *3*, 554.
(22) Cole, K. C.; Gu'evremont, J.; Ajji, A.; Dumoulin, M. M. *Appl. Spectrosc.* **1994**, *48*, 1513.
(23) Watanabe, J.; Hayashi, M. *Macromolecules* **1988**, *21*, 278; **1989**, *22*, 4083.
(24) Tokita, M.; Osada, K.; Watanabe, J. *Liq. Cryst.* **1998**, *24*, 477.
(25) Watanabe, J.; Kinoshita, S. *J. Phys. II* **1992**, *2*, 1273.
(26) Tokita, M.; Takahashi, T.; Hayashi, M.; Watanabe, J. *Macromolecules* **1996**, *29*, 1345.
(27) Watanabe, J.; Hayashi, M.; Morita, A.; Tokita, M. *Macromolecules* **1995**, *28*, 8073.
(28) Gutiérrez, M. C. G.; Karger-Kocsis, J.; Riekel, C. *Macromolecules* **2002**, *35*, 7320.
(29) Ran, S.; Wang, Z.; Burger, C.; Chu, B.; Hsiao, B. S. *Macromolecules* **2002**, *35*, 10102.
(30) Carr, P. L.; Nicholson, T. M.; Ward, I. M. *Polym. Adv. Technol.* **1997**, *8*, 592.
(31) Auriemmam, F.; Corradini, P.; Rosa, De C.; Gureera, G.; Petraccone, V.; Biachi, Riccardo; Dino, Di. G. *Macromolecules* **1992**, *25*, 2490.
(32) Welsh, G. E.; Blundell, D. J.; Windle, A. H. *Macromolecules* **1998**, *31*, 7562.

MA0486905